Journal of Structural Dynamics, 4, (pp. 45-57) 2026
A mixed admittance/transfer matrix substructuring approach

Journal of Structural Dynamics

A mixed admittance/transfer matrix substructuring approach

J W R Meggitt *[1]

[1] *Acoustics Research Centre, University of Salford, Greater Manchester, England*

Abstract

Substructuring is an important step in the analysis of complex built-up structures. It is the process by which individual components are mathematically assembled to build a model of a coupled system. In the frequency domain, admittance or FRF-based substructuring has become the preferred approach, especially when considering experimental components for which FRFs are easily obtained from test data. However, FRFs are not the only way to represent a component in the frequency domain. Often, particularly for layered systems, the so-called *transfer matrix* (TM) representation becomes more convenient; component coupling is achieved by simply multiplying together their respective TMs. In the present paper we develop a hybrid substructuring scheme that allows the coupling of FRF-based components using a TM representation of the interconnecting junction. Such an approach might be beneficial for structures with complex layered connections (well suited to TM-based coupling), and has the potential to provide additional insight into structural transmission through multiple interconnected elements.

Keywords: Substructuring; transfer matrix method; frequency response functions; admittance coupling

Received on August 14, 2025, Accepted on January 5, 2026, Published on January 9, 2026

1 Introduction

To analyse the vibro-acoustic performance of a complex built-up structure it is convenient to adopt a component-based approach [1]. The assembly is decomposed into a series of interconnecting components which are independently characterised, either by experiment or numerically. These component representations are then combined mathematically to yield a model of the assembled system, a process termed substructuring. The process of substructuring amounts to the enforcement of compatibility and equilibrium between the connecting degrees of freedom (DoFs) of each component. This can be achieved in a variety of ways, and in any of the domains typically used for structural dynamic analysis, including the physical, modal, state, time and frequency domains [2]. In recent years, frequency domain methods have gained popularity, given the ease of which they allow for combining experimental and numerical component representations.

In the frequency domain, components are most often represented by their *free-interface admittance* matrices, which describe their kinematic response due to a set of applied forces. Based on component admittance, various substructuring schemes are available, including direct [1], primal/dual [2] and mixed [3] formulations. The advantage of an admittance-based approach, is the relative ease in which the component admittance matrices can be measured. It is not however the only approach available. An alternative frequency domain representation is by the so-called *transfer matrix* [4], which relates the state vector (stacked force and response) between two sets of DoFs, usually considered the input and output of the component. The advantage of a transfer matrix approach is that structural coupling of two of more components is reduced to a simple multiplication of their respective transfer matrices. This is especially convenient for modeling systems where the components form a cascaded chain, such as when dealing with layered materials [5, 6].

*j.w.r.meggitt1@salford.ac.uk

The transfer matrix method (TMM) has found greatest application in acoustics, where it is used extensively to model sound transmission through multi-layered structures [7, 8, 9], though applications also exist in structural dynamics and vibration. For example, in [10] and [11] the authors use the TMM to model the dynamics of beams with variable cross-sections. In [12] the TMM is used as an analytical tool to study the vibration of compressed helical springs. In [13] and [14] the TMM is applied to the study of rotor-bearing systems comprising coupled lateral and torsional vibration and local/global coupler offsets. In [15] TMs are used to analyse the vibrational power flow through a MIMO system.

The TMM has also been incorporated within other modeling schemes to provide an efficient inclusion of layered materials/structures. In [16] the hybridisation of Finite Element and TMM is proposed for the efficient analysis of plate and shell structures. In [17] the TMM is combined with hybrid FEA-SEA method for diffuse sound transmission through finite-sized thick and layered wall and floor systems. In [18] the coupling of TMM and Finite Element method is used for the efficient acoustic analysis of automotive hollow body networks. The TM representation also forms the basis of the so-called Wave-FE approach used for efficient modeling of periodic structures [19].

In this paper we present a mixed admittance/transfer matrix-based substructuring scheme. We consider the problem depicted in Figure 1 (though the proposed scheme can readily be generalised to more complex systems), where two admittance-based components are coupled by a series of connecting elements which together form a *junction*. We wish to represent the dynamics of this layered junction by the more convenient transfer matrix, whilst keeping the end components in their admittance form. The result is a generalization of the dual formulation for admittance-based substructuring, where the conditions of equilibrium and compatibility between components are replaced by the junction transfer matrix equations, themselves built from an arbitrary number of sub-element transfer matrices. The principle advantage of the proposed approach is the ease of which complex layered systems can be incorporated within an admittance substructuring scheme. Adding, removing, or reordering junction components is achieved by directly including, removing, or reordering their respective transfer matrices, thus avoiding the need to redefine the Boolean coupling matrices required by the conventional dual formulation.

Having outlined the context of this paper, its remainder will be structured as follows. In Section 2 we introduce the admittance and transfer matrix methods for structural coupling. Following this in Section 3, we present the mixed admittance-transfer matrix substructuring scheme with a simple numerical example in Section 4. Finally, Section 5 draws some concluding remarks.

2 Structural coupling

In this section we introduce the admittance and transfer matrix-based substructuring methods that we wish to combine into a common framework. The principal difference between these two methods is in how they represent the dynamics of their respective substructures (described below). Irrespective of this representation, the rigid coupling of two components is governed by the conditions of compatibility and equilibrium,

$$\mathbf{u}_1 = \mathbf{u}_2 \qquad \mathbf{g}_1 = -\mathbf{g}_2 \tag{1}$$

which state that when two components are in rigid contact their interface DoFs must a) have the same kinematic response (displacement, velocity and acceleration) and b) exert equal and opposite forces onto one another. Depending on the chosen domain and/or component representation, the methods for enforcing these constraints will differ.

2.1 Admittance-based (FRF) coupling

With admittance-based substructuring, each component is represented by a complex admittance matrix $\mathbf{Y}^{(n)}$ that satisfies the equation of motion (per frequency),

$$\mathbf{u}^{(n)} = \mathbf{Y}^{(n)}(\mathbf{f}^{(n)} + \mathbf{g}^{(n)}) \tag{2}$$

where $\mathbf{f}$ and $\mathbf{g}$ are, respectively, the externally applied and interface coupling forces that act on the component, and $\mathbf{u}$ is its kinematic response (displacement, velocity or acceleration depending on the units of $\mathbf{Y}$).

To model an assembly of P such components, we begin by writing their equations of motion in a block diagonal form,

$$\mathbf{u} = \mathbf{Y}\,(\mathbf{f} + \mathbf{g}) \tag{3}$$

where, $\mathbf{Y}$ is the block diagonal admittance matrix of the P uncoupled components, $\mathbf{u}$ is the corresponding block vector of responses, $\mathbf{f}$ is the block vector of applied forces, and $\mathbf{g}$ the block vector of interface coupling forces,

$$\mathbf{Y} = \begin{bmatrix} \mathbf{Y}^{(1)} & & & \\ & \mathbf{Y}^{(2)} & & \\ & & \ddots & \\ & & & \mathbf{Y}^{(P)} \end{bmatrix}, \quad \mathbf{u} = \begin{pmatrix} \mathbf{u}^{(1)} \\ \mathbf{u}^{(2)} \\ \vdots \\ \mathbf{u}^{(P)} \end{pmatrix}, \quad \mathbf{f} = \begin{pmatrix} \mathbf{f}^{(1)} \\ \mathbf{f}^{(2)} \\ \vdots \\ \mathbf{f}^{(P)} \end{pmatrix}, \quad \mathbf{g} = \begin{pmatrix} \mathbf{g}^{(1)} \\ \mathbf{g}^{(2)} \\ \vdots \\ \mathbf{g}^{(P)} \end{pmatrix}.$$

To rigidly couple the connecting components, the conditions of compatibility and equilibrium must be satisfied across the set of co-located coupling DoFs. To aid flexible DoF selection, compatibility and equilibrium are expressed in the general matrix form,

$$\mathbf{B}\mathbf{u} = \mathbf{0}, \tag{4}$$

and

$$\mathbf{L}^{\mathrm{T}}\mathbf{g} = \mathbf{0} \tag{5}$$

where $\mathbf{B}$ and $\mathbf{L}^{\mathrm{T}}$ are signed and unsigned Boolean matrices that specify *which* DoFs are to be coupled [2]. Equations 3, 4 and 5 are commonly referred to as the *three field formulation*.

The rigid coupling of two components implies the internal forces are of equal magnitude (or intensity) and opposite direction. Hence, we are able to define *a priori* the form of $\mathbf{g}$ as,

$$\mathbf{g} = -\mathbf{B}^{\mathrm{T}}\lambda \tag{6}$$

where $\mathbf{B}$ prescribes the equal and opposite signage, and λ is a vector of interface force magnitudes. Combining equation 5 and 6, we see that $\mathbf{L}^{\mathrm{T}}$ and $\mathbf{B}^{\mathrm{T}}$ represent the null-space of one another, since we must have $-\mathbf{L}^{\mathrm{T}}\mathbf{B}^{\mathrm{T}}\lambda = \mathbf{0}$ for any value of λ.

Substituting $\mathbf{g}$ into the block equations of motion we have,

$$\mathbf{u} = \mathbf{Y}\left(\mathbf{f} - \mathbf{B}^{\mathrm{T}}\lambda\right). \tag{7}$$

To determine the coupled assembly response, we first find the interface force required to bring the system into alignment (i.e. satisfy equation 4). To do so we substitute equation 7 into the compatibility equation,

$$\mathbf{B}\mathbf{u} = \mathbf{B}\mathbf{Y}\left(\mathbf{f} - \mathbf{B}^{\mathrm{T}}\lambda\right) = \mathbf{B}\mathbf{Y}\mathbf{f} - \mathbf{B}\mathbf{Y}\mathbf{B}^{\mathrm{T}}\lambda = \mathbf{0}, \tag{8}$$

before rearranging to solve for λ,

$$\lambda = \left(\mathbf{B}\mathbf{Y}\mathbf{B}^{\mathrm{T}}\right)^{-1}\mathbf{B}\mathbf{Y}\mathbf{f}. \tag{9}$$

We can now substitute λ back into the equations of motion to yield the coupled response,

$$\mathbf{u} = \mathbf{Y}\left(\mathbf{f} - \mathbf{B}^{\mathrm{T}}\left(\mathbf{B}\mathbf{Y}\mathbf{B}^{\mathrm{T}}\right)^{-1}\mathbf{B}\mathbf{Y}\mathbf{f}\right) = \left(\mathbf{Y} - \mathbf{Y}\mathbf{B}^{\mathrm{T}}\left(\mathbf{B}\mathbf{Y}\mathbf{B}^{\mathrm{T}}\right)^{-1}\mathbf{B}\mathbf{Y}\right)\mathbf{f}. \tag{10}$$

From the above we can identify the coupled admittance as,

$$\mathbf{Y}_C = \mathbf{Y} - \mathbf{Y}\mathbf{B}^{\mathrm{T}}\left(\mathbf{B}\mathbf{Y}\mathbf{B}^{\mathrm{T}}\right)^{-1}\mathbf{B}\mathbf{Y}. \tag{11}$$

Equation 11 provides a convenient framework for general substructuring; it allows an arbitrary number of components to be assembled in any configuration, and avoids large matrix inversions typical of other admittance-based formulations.

2.2 Transfer matrix-based (TM) coupling

With transfer matrix-based coupling, each component is represented by a complex transfer matrix $\mathbf{T}$ that relates the force and response between two sets of DoFs (say c_1 and c_2),

$$\begin{pmatrix} \mathbf{u}_{c_2} \\ \mathbf{f}_{c_2} - \mathbf{g}_{c_2} \end{pmatrix} = \overbrace{\begin{bmatrix} \mathbf{T}^u & \mathbf{\Gamma} \\ \mathbf{\Omega} & \mathbf{T}^g \end{bmatrix}}^{\mathbf{T}} \begin{pmatrix} \mathbf{u}_{c_1} \\ \mathbf{f}_{c_1} + \mathbf{g}_{c_1} \end{pmatrix}. \tag{12}$$

Within the transfer matrix, the submatrices $\mathbf{T}^g$ and $\mathbf{T}^u$ represent a pair of force and response transmissibilities. Whilst transmissibilities have many interesting properties and applications, they do not themselves fully characterize a component [20]. The off-diagonal terms $\mathbf{\Gamma}$ and $\mathbf{\Omega}$ provide the necessary force-response cross-terms required for the transfer matrix representation of a component to be complete (see Appendix A).

To rigidly couple two components A and B,

$$\begin{pmatrix} \mathbf{u}_{Ac_2} \\ -\mathbf{g}_{Ac_2} \end{pmatrix} = \begin{bmatrix} \mathbf{T}^u_A & \mathbf{\Gamma}_A \\ \mathbf{\Omega}_A & \mathbf{T}^g_A \end{bmatrix} \begin{pmatrix} \mathbf{u}_{Ac_1} \\ \mathbf{g}_{Ac_1} \end{pmatrix} \qquad \begin{pmatrix} \mathbf{u}_{Bc_3} \\ -\mathbf{g}_{Bc_3} \end{pmatrix} = \begin{bmatrix} \mathbf{T}^u_B & \mathbf{\Gamma}_B \\ \mathbf{\Omega}_B & \mathbf{T}^g_B \end{bmatrix} \begin{pmatrix} \mathbf{u}_{Bc_2} \\ \mathbf{g}_{Bc_2} \end{pmatrix}. \tag{13}$$

through the DoFs c_2 we simply recall the conditions of compatibility and equilibrium,

$$\begin{pmatrix} \mathbf{u}_{Ac_2} \\ -\mathbf{g}_{Ac_2} \end{pmatrix} = \begin{pmatrix} \mathbf{u}_{Bc_2} \\ \mathbf{g}_{Bc_2} \end{pmatrix} \tag{14}$$

and combine equation 13 as so,

$$\begin{pmatrix} \mathbf{u}_{Bc_3} \\ -\mathbf{g}_{Bc_3} \end{pmatrix} = \begin{bmatrix} \mathbf{T}^u_B & \mathbf{\Gamma}_B \\ \mathbf{\Omega}_B & \mathbf{T}^g_B \end{bmatrix} \begin{bmatrix} \mathbf{T}^u_A & \mathbf{\Gamma}_A \\ \mathbf{\Omega}_A & \mathbf{T}^g_A \end{bmatrix} \begin{pmatrix} \mathbf{u}_{Ac_1} \\ \mathbf{g}_{Ac_1} \end{pmatrix}. \tag{15}$$

Clearly, this approach to coupling can be extended for an arbitrary number of components,

$$\begin{pmatrix} \mathbf{u}_{Nc_{N+1}} \\ -\mathbf{g}_{Nc_{N+1}} \end{pmatrix} = \begin{bmatrix} \mathbf{T}^u_N & \mathbf{\Gamma}_N \\ \mathbf{\Omega}_N & \mathbf{T}^g_N \end{bmatrix} \begin{bmatrix} \mathbf{T}^u_M & \mathbf{\Gamma}_M \\ \mathbf{\Omega}_M & \mathbf{T}^g_M \end{bmatrix} \cdots \begin{bmatrix} \mathbf{T}^u_B & \mathbf{\Gamma}_B \\ \mathbf{\Omega}_B & \mathbf{T}^g_B \end{bmatrix} \begin{bmatrix} \mathbf{T}^u_A & \mathbf{\Gamma}_A \\ \mathbf{\Omega}_A & \mathbf{T}^g_A \end{bmatrix} \begin{pmatrix} \mathbf{u}_{Ac_1} \\ \mathbf{g}_{Ac_1} \end{pmatrix} \tag{16}$$

$$= \begin{bmatrix} \mathbf{T}^u_{N\cdots A} & \mathbf{\Gamma}_{N\cdots A} \\ \mathbf{\Omega}_{N\cdots A} & \mathbf{T}^g_{N\cdots A} \end{bmatrix} \begin{pmatrix} \mathbf{u}_{Ac_1} \\ \mathbf{g}_{Ac_1} \end{pmatrix}. \tag{17}$$

This is especially useful for complex layered structures, where each layer is simply represented by its own transfer matrix. In addition to providing convenient structural coupling, the transfer matrix $\mathbf{T}$ can be used to derive and inspect the free wave characteristics of a component (or collection thereof), as done by the WFE method [19].

2.2.1 Experimental characeterisation of transfer matrices

The direct measurement of a component's transfer matrix, whilst possible in theory, is not a straightforward task. This is because it would require rigidly constraining the junction DoFs to obtain certain terms, for example the force transmissibility $\mathbf{T}^g$, which is defined element-wise as,

$$T^g_{c_{1,i},c_{2,j}} = \left.\frac{-g_{c_{2,i}}}{g_{c_{1,j}}}\right|_{\mathbf{u}_{c_1}=\mathbf{0},\,\mathbf{g}_{c_{1,k\neq j}}=\mathbf{0}} \tag{18}$$

requires the constraint $\mathbf{u}_{c_1} = \mathbf{0}$. In practice, it is more convenient to measure the component's admittance matrix at and between the two coupling DoF sets, and then convert these to a transfer matrix representation using (see appendix A for details),

$$\begin{pmatrix} \mathbf{u}_{c_2} \\ -\mathbf{g}_{c_2} \end{pmatrix} = \begin{bmatrix} \mathbf{T}^u & \mathbf{\Gamma} \\ \mathbf{\Omega} & \mathbf{T}^g \end{bmatrix} \begin{pmatrix} \mathbf{u}_{c_1} \\ \mathbf{g}_{c_1} \end{pmatrix} = \begin{bmatrix} \mathbf{Y}_{c_2c_2}\mathbf{Y}^{-1}_{c_1c_2} & \mathbf{Y}_{c_2c_1} - \mathbf{Y}_{c_2c_2}\mathbf{Y}^{-1}_{c_1c_2}\mathbf{Y}_{c_1c_1} \\ -\mathbf{Y}^{-1}_{c_1c_2} & \mathbf{Y}^{-1}_{c_1c_2}\mathbf{Y}_{c_1c_1} \end{bmatrix} \begin{pmatrix} \mathbf{u}_{c_1} \\ \mathbf{g}_{c_1} \end{pmatrix}. \tag{19}$$

3 Hybrid Admittance-TM coupling

We wish to combine the admittance and transfer matrix coupling schemes describe above, to model systems of the form shown in Figure 1, where the junction between two admittance components is represented by a general transfer matrix.

In the proposed hybrid substructuring scheme, the coupling conditions (i.e. equilibrium and compatibility) between two admittance-based components (A and B) are replaced by the transfer matrix of a coupling junction J,

$$\begin{pmatrix} \mathbf{u}_{c_2} \\ -\mathbf{g}_{c_2} \end{pmatrix} = \begin{bmatrix} \mathbf{T}^u_J & \mathbf{\Gamma}_J \\ \mathbf{\Omega}_J & \mathbf{T}^g_J \end{bmatrix} \begin{pmatrix} \mathbf{u}_{c_1} \\ \mathbf{g}_{c_1} \end{pmatrix}. \tag{20}$$

This junction might represent something as simple as a spring-like connection, or instead a more complex chain of components (assembled from their individual transfer matrices as per equation 16).

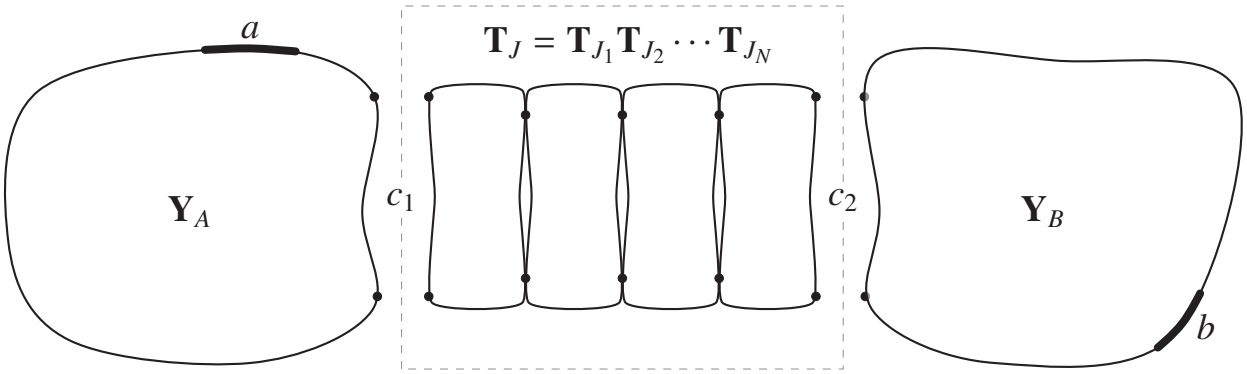

Fig. 1: Hybrid substructuring model; components A and B are represented by their admittance matrices $\mathbf{Y}_A$ and $\mathbf{Y}_B$, junction J is characterised by the transfer matrix $\mathbf{T}_J$.

From equation 20 we have,

$$\mathbf{u}_{c_2} = \mathbf{T}_u\mathbf{u}_{c_1} + \mathbf{\Gamma}\mathbf{g}_{c_1} \tag{21}$$

and

$$-\mathbf{g}_{c_2} = \mathbf{\Omega}\mathbf{u}_{c_1} + \mathbf{T}_g\mathbf{g}_{c_1} \tag{22}$$

where for clarity the subscript J has been omitted and u and g made into subscripts. We extend equation 21 and 22 to include the internal A and B DoFs (denoted a and b), and rewrite them in a form reminiscent of equations 4 and 5,

$$\mathbf{0} = \begin{bmatrix} \mathbf{0} & \mathbf{T}_u & -\mathbf{I} & \mathbf{0} \end{bmatrix}\begin{Bmatrix} \mathbf{u}_a \\ \mathbf{u}_{c_1} \\ \mathbf{u}_{c_2} \\ \mathbf{u}_b \end{Bmatrix} + \begin{bmatrix} \mathbf{0} & \mathbf{\Gamma} & \mathbf{0} & \mathbf{0} \end{bmatrix}\begin{bmatrix} \mathbf{g}_a \\ \mathbf{g}_{c_1} \\ \mathbf{g}_{c_2} \\ \mathbf{g}_b \end{bmatrix} = \mathbf{B}_u\mathbf{u} + \bar{\mathbf{\Gamma}}\mathbf{g} = \mathbf{0} \tag{23}$$

and

$$\mathbf{0} = \begin{bmatrix} \mathbf{I} & \mathbf{0} & \mathbf{0} & \mathbf{0} \\ \mathbf{0} & \mathbf{T}_g & \mathbf{I} & \mathbf{0} \\ \mathbf{0} & \mathbf{0} & \mathbf{0} & \mathbf{I} \end{bmatrix}\begin{bmatrix} \mathbf{g}_a \\ \mathbf{g}_{c_1} \\ \mathbf{g}_{c_2} \\ \mathbf{g}_b \end{bmatrix} + \begin{bmatrix} \mathbf{0} & \mathbf{0} & \mathbf{0} & \mathbf{0} \\ \mathbf{0} & \mathbf{\Omega} & \mathbf{0} & \mathbf{0} \\ \mathbf{0} & \mathbf{0} & \mathbf{0} & \mathbf{0} \end{bmatrix}\begin{bmatrix} \mathbf{u}_a \\ \mathbf{u}_{c_1} \\ \mathbf{u}_{c_2} \\ \mathbf{u}_b \end{bmatrix} = \mathbf{L}_g^{\mathrm{T}}\mathbf{g} + \bar{\mathbf{\Omega}}\mathbf{u} = \mathbf{0}, \tag{24}$$

where we introduce $\mathbf{B}_u$ and $\mathbf{L}_g^{\mathrm{T}}$ to represent the response-to-response and force-to-force relations across the junction. Note that in contrast to standard admittance-based substructuring scheme $\mathbf{B}_u$ and $\mathbf{L}_g^{\mathrm{T}}$ are no longer signed/unsigned Boolean matrices that simply equate the force and response; they now include transmissibility functions that partition the force and response according to the dynamics of the connecting junction. To provide a complete description of the junction, the force-to-response ($\bar{\mathbf{\Gamma}}$) and response-to-force ($\bar{\mathbf{\Omega}}$) contributions are also be included.

From the above we can establish a *modified three field formulation* for a hybrid assembly that includes a coupling junction represented by a general transfer matrix:

$$\mathbf{u} = \mathbf{Y}(\mathbf{f} + \mathbf{g}) \tag{25}$$

$$\mathbf{0} = \mathbf{B}_u\mathbf{u} + \bar{\mathbf{\Gamma}}\mathbf{g} \tag{26}$$

$$\mathbf{0} = \mathbf{L}_g^{\mathrm{T}}\mathbf{g} + \bar{\mathbf{\Omega}}\mathbf{u} \tag{27}$$

with,

$$\mathbf{Y} = \begin{bmatrix} \mathbf{Y}_A & \\ & \mathbf{Y}_B \end{bmatrix}, \quad \mathbf{u} = \begin{Bmatrix} \mathbf{u}_A \\ \mathbf{u}_B \end{Bmatrix} = \begin{Bmatrix} \mathbf{u}_a \\ \mathbf{u}_{c_1} \\ \mathbf{u}_{c_2} \\ \mathbf{u}_b \end{Bmatrix}, \quad \mathbf{g} = \begin{Bmatrix} \mathbf{g}_A \\ \mathbf{g}_B \end{Bmatrix} = \begin{Bmatrix} \mathbf{g}_a \\ \mathbf{g}_{c_1} \\ \mathbf{g}_{c_2} \\ \mathbf{g}_b \end{Bmatrix}, \quad \mathbf{f} = \begin{Bmatrix} \mathbf{f}_A \\ \mathbf{f}_B \end{Bmatrix} = \begin{Bmatrix} \mathbf{f}_a \\ \mathbf{f}_{c_1} \\ \mathbf{f}_{c_2} \\ \mathbf{f}_b \end{Bmatrix}. \tag{28}$$

In effect, we have introduced a pair of *dynamic* compatibility and equilibrium conditions which describe the dynamics of the coupling junction. At this point, we proceed in a manner similar to the admittance-based derivation.

Note that in contrast to the standard formulation, our force and response constraints are now coupled. We can no longer assume the form of $\mathbf{g} = -\mathbf{B}^{\mathrm{T}}\lambda$, since force conservation is not guaranteed across an arbitrary junction. Hence, we must determine a form of $\mathbf{g}$ that satisfies equation 27. An appropriate form is given by,

$$\mathbf{g} = -\begin{bmatrix} \mathbf{0} \\ -\mathbf{I} \\ \mathbf{T}_g \\ \mathbf{0} \end{bmatrix}\lambda - \begin{bmatrix} \mathbf{0} & \mathbf{0} & \mathbf{0} & \mathbf{0} \\ \mathbf{0} & \mathbf{0} & \mathbf{0} & \mathbf{0} \\ \mathbf{0} & \boldsymbol{\Omega} & \mathbf{0} & \mathbf{0} \\ \mathbf{0} & \mathbf{0} & \mathbf{0} & \mathbf{0} \end{bmatrix}\mathbf{u} = -\mathbf{B}_g^{\mathrm{T}}\lambda - \bar{\bar{\boldsymbol{\Omega}}}\mathbf{u} \tag{29}$$

where as in the standard dual formulation λ are a set of Lagrange multipliers representing interface force magnitudes. Equation 29 can be verified by substituting it into equation 27. In doing so, we see that $\mathbf{B}_g$ continues to represent the null-space of $\mathbf{L}_g$ (and vise versa), since by construction we have that $-\mathbf{L}_g^{\mathrm{T}}\mathbf{B}_g^{\mathrm{T}}\lambda = \mathbf{0}$.

Note that the form of $\mathbf{g}$ above differs from the standard dual formulation in two ways: 1) a force transmissibility replaces what was an identity matrix; this facilitates a change in force across the junction, and 2) the introduction of a response dependent contribution to the interface force.

Substituting $\mathbf{g}$ into the equation of motion as represented by equation 25 and isolating $\mathbf{u}$, the coupling problem is reduced to,

$$\mathbf{u} = \mathbf{Y}\left(\mathbf{f} - \mathbf{B}_g^{\mathrm{T}}\lambda - \bar{\bar{\boldsymbol{\Omega}}}\mathbf{u}\right) = \left(\mathbf{I} + \mathbf{Y}\bar{\bar{\boldsymbol{\Omega}}}\right)^{-1}\mathbf{Y}\left(\mathbf{f} - \mathbf{B}_g^{\mathrm{T}}\lambda\right) \tag{30}$$

$$\mathbf{0} = \mathbf{B}_u\mathbf{u} + \bar{\boldsymbol{\Gamma}}\mathbf{g} \tag{31}$$

As before, to determine the coupled admittance we must find λ. We begin by substituting $\mathbf{g}$ into equation 31,

$$\mathbf{B}_u\mathbf{u} + \bar{\boldsymbol{\Gamma}}\mathbf{g} = \mathbf{B}_u\mathbf{u} + \bar{\boldsymbol{\Gamma}}\left(-\mathbf{B}_g^{\mathrm{T}}\lambda - \bar{\bar{\boldsymbol{\Omega}}}\mathbf{u}\right) = \mathbf{0}. \tag{32}$$

Factoring out $\mathbf{u}$,

$$\mathbf{B}_u\mathbf{u} - \bar{\boldsymbol{\Gamma}}\mathbf{B}_g^{\mathrm{T}}\lambda - \bar{\boldsymbol{\Gamma}}\bar{\bar{\boldsymbol{\Omega}}}\mathbf{u} = \left(\mathbf{B}_u - \bar{\boldsymbol{\Gamma}}\bar{\bar{\boldsymbol{\Omega}}}\right)\mathbf{u} - \bar{\boldsymbol{\Gamma}}\mathbf{B}_g^{\mathrm{T}}\lambda = \mathbf{0} \tag{33}$$

and substituting in equation 30 yields,

$$\left(\mathbf{B}_u - \bar{\boldsymbol{\Gamma}}\bar{\bar{\boldsymbol{\Omega}}}\right)\left(\mathbf{I} + \mathbf{Y}\bar{\bar{\boldsymbol{\Omega}}}\right)^{-1}\mathbf{Y}\left(\mathbf{f} - \mathbf{B}_g^{\mathrm{T}}\lambda\right) - \bar{\boldsymbol{\Gamma}}\mathbf{B}_g^{\mathrm{T}}\lambda = \mathbf{0}. \tag{34}$$

Factoring out λ,

$$\left(\mathbf{B}_u - \bar{\boldsymbol{\Gamma}}\bar{\bar{\boldsymbol{\Omega}}}\right)\left(\mathbf{I} + \mathbf{Y}\bar{\bar{\boldsymbol{\Omega}}}\right)^{-1}\mathbf{Y}\mathbf{f} - \left[\left(\mathbf{B}_u - \bar{\boldsymbol{\Gamma}}\bar{\bar{\boldsymbol{\Omega}}}\right)\left(\mathbf{I} + \mathbf{Y}\bar{\bar{\boldsymbol{\Omega}}}\right)^{-1}\mathbf{Y}\mathbf{B}_g^{\mathrm{T}} + \bar{\boldsymbol{\Gamma}}\mathbf{B}_g^{\mathrm{T}}\right]\lambda = \mathbf{0} \tag{35}$$

moving the first term to the right-hand-side, and pre-multiplying by the inverse of the square bracket, we obtain,

$$\lambda = \left[\left(\mathbf{B}_u - \bar{\boldsymbol{\Gamma}}\bar{\bar{\boldsymbol{\Omega}}}\right)\left(\mathbf{I} + \mathbf{Y}\bar{\bar{\boldsymbol{\Omega}}}\right)^{-1}\mathbf{Y}\mathbf{B}_g^{\mathrm{T}} + \bar{\boldsymbol{\Gamma}}\mathbf{B}_g^{\mathrm{T}}\right]^{-1}\left(\mathbf{B}_u - \bar{\boldsymbol{\Gamma}}\bar{\bar{\boldsymbol{\Omega}}}\right)\left(\mathbf{I} + \mathbf{Y}\bar{\boldsymbol{\Omega}}\right)^{-1}\mathbf{Y}\mathbf{f}. \tag{36}$$

We can now substitute λ back into equation 30 to yield the coupled assembly response,

$$\mathbf{u} = \left(\mathbf{I} + \mathbf{Y}\bar{\bar{\boldsymbol{\Omega}}}\right)^{-1}\mathbf{Y}\left(\mathbf{I} - \mathbf{B}_g^{\mathrm{T}}\left[\left(\mathbf{B}_u - \bar{\boldsymbol{\Gamma}}\bar{\bar{\boldsymbol{\Omega}}}\right)\left(\mathbf{I} + \mathbf{Y}\bar{\bar{\boldsymbol{\Omega}}}\right)^{-1}\mathbf{Y}\mathbf{B}_g^{\mathrm{T}} + \bar{\boldsymbol{\Gamma}}\mathbf{B}_g^{\mathrm{T}}\right]^{-1}\left(\mathbf{B}_u - \bar{\boldsymbol{\Gamma}}\bar{\bar{\boldsymbol{\Omega}}}\right)\left(\mathbf{I} + \mathbf{Y}\bar{\bar{\boldsymbol{\Omega}}}\right)^{-1}\mathbf{Y}\right)\mathbf{f}. \tag{37}$$

From inspection we can see that $\bar{\boldsymbol{\Gamma}}\bar{\bar{\boldsymbol{\Omega}}} = \mathbf{0}$ and $\bar{\boldsymbol{\Gamma}}\mathbf{B}_g^{\mathrm{T}} = -\boldsymbol{\Gamma}$. Finally, from the above we have the coupled assembly admittance,

$$\mathbf{Y}_C = \left(\mathbf{I} + \mathbf{Y}\bar{\bar{\boldsymbol{\Omega}}}\right)^{-1}\mathbf{Y} - \left(\mathbf{I} + \mathbf{Y}\bar{\bar{\boldsymbol{\Omega}}}\right)^{-1}\mathbf{Y}\mathbf{B}_g^{\mathrm{T}}\left[\mathbf{B}_u\left(\mathbf{I} + \mathbf{Y}\bar{\bar{\boldsymbol{\Omega}}}\right)^{-1}\mathbf{Y}\mathbf{B}_g^{\mathrm{T}} - \boldsymbol{\Gamma}\right]^{-1}\mathbf{B}_u\left(\mathbf{I} + \mathbf{Y}\bar{\bar{\boldsymbol{\Omega}}}\right)^{-1}\mathbf{Y} \tag{38}$$

with,

$$\mathbf{B}_g^{\mathrm{T}} = \begin{bmatrix} \mathbf{0} \\ -\mathbf{I} \\ \mathbf{T}_g \\ \mathbf{0} \end{bmatrix}, \quad \mathbf{B}_u = \begin{bmatrix} \mathbf{0} & \mathbf{T}_u & -\mathbf{I} & \mathbf{0} \end{bmatrix}, \quad \text{and} \quad \bar{\bar{\boldsymbol{\Omega}}} = \begin{bmatrix} \mathbf{0} & \mathbf{0} & \mathbf{0} & \mathbf{0} \\ \mathbf{0} & \mathbf{0} & \mathbf{0} & \mathbf{0} \\ \mathbf{0} & \boldsymbol{\Omega} & \mathbf{0} & \mathbf{0} \\ \mathbf{0} & \mathbf{0} & \mathbf{0} & \mathbf{0} \end{bmatrix} \tag{39}$$

Equations 38-39 describe the admittance of the coupled AJB assembly, with the components A and B being represented by their respective admittance matrices, and the junction J by its transfer matrix,

$$\mathbf{Y} = \begin{bmatrix} \mathbf{Y}_A & \\ & \mathbf{Y}_B \end{bmatrix}, \qquad \mathbf{T}_J = \begin{bmatrix} \mathbf{T}_u & \boldsymbol{\Gamma} \\ \boldsymbol{\Omega} & \mathbf{T}_g \end{bmatrix}. \tag{40}$$

Note that in equation 38 only the DoFs of A and B are present; those within the layered junction are not. Instead, the effect of the junction is treated similarly to a static joint, through the *dynamic* compatibility/equilibrium conditions in equation 26-27.

To verify equations 38 and 39 we can consider two basic junction types: a rigid connection and a massless spring-damper.

Rigid junction The transfer matrix of a rigid junction is given by,

$$\begin{pmatrix} \mathbf{u}_{c_2} \\ -\mathbf{g}_{c_2} \end{pmatrix} = \begin{bmatrix} \mathbf{I} & \mathbf{0} \\ \mathbf{0} & \mathbf{I} \end{bmatrix} \begin{pmatrix} \mathbf{u}_{c_1} \\ \mathbf{g}_{c_1} \end{pmatrix} \tag{41}$$

from which we have,

$$\mathbf{B}_g^{\mathrm{T}} = \begin{bmatrix} \mathbf{0} \\ -\mathbf{I} \\ \mathbf{I} \\ \mathbf{0} \end{bmatrix}, \quad \mathbf{B}_u = \begin{bmatrix} \mathbf{0} & \mathbf{I} & -\mathbf{I} & \mathbf{0} \end{bmatrix}, \quad \boldsymbol{\Gamma} = \begin{bmatrix} \mathbf{0} & \mathbf{0} & \mathbf{0} & \mathbf{0} \end{bmatrix}, \quad \bar{\bar{\boldsymbol{\Omega}}} = \begin{bmatrix} \mathbf{0} & \mathbf{0} & \mathbf{0} & \mathbf{0} \\ \mathbf{0} & \mathbf{0} & \mathbf{0} & \mathbf{0} \\ \mathbf{0} & \mathbf{0} & \mathbf{0} & \mathbf{0} \\ \mathbf{0} & \mathbf{0} & \mathbf{0} & \mathbf{0} \end{bmatrix}. \tag{42}$$

Based on the above, we see that equation 38 reduces to,

$$\mathbf{Y}_C = \mathbf{Y} - \mathbf{Y}\mathbf{B}^{\mathrm{T}} \left[\mathbf{B}\mathbf{Y}\mathbf{B}^{\mathrm{T}}\right]^{-1} \mathbf{B}\mathbf{Y} \tag{43}$$

which is standard admittance-based coupling.

Spring damper junction Taking $\mathbf{u}$ as structural velocity (such that $\mathbf{Y}$ and $\mathbf{Z}$ become mobility and impedance, respectively) the transfer matrix of an idealised spring-damper junction with stiffness K and damping C is given by,

$$\begin{pmatrix} \mathbf{u}_{c_2} \\ -\mathbf{g}_{c_2} \end{pmatrix} = \begin{bmatrix} -\mathbf{Z}_{c_1c_2}^{-1}\mathbf{Z}_{c_1c_1} & \mathbf{Z}_{c_1c_2}^{-1} \\ -\mathbf{Z}_{c_2c_1} + \mathbf{Z}_{c_2c_2}\mathbf{Z}_{c_1c_2}^{-1}\mathbf{Z}_{c_1c_1} & -\mathbf{Z}_{c_2c_2}\mathbf{Z}_{c_1c_2}^{-1} \end{bmatrix} \begin{pmatrix} \mathbf{u}_{c_1} \\ \mathbf{g}_{c_1} \end{pmatrix} = \begin{bmatrix} \mathbf{I} & -\mathrm{diag}\left(\frac{K}{j\omega} + C\right)^{-1} \\ \mathbf{0} & \mathbf{I} \end{bmatrix} \begin{pmatrix} \mathbf{u}_{c_1} \\ \mathbf{g}_{c_1} \end{pmatrix} \tag{44}$$

from which we have,

$$\mathbf{B}_g^{\mathrm{T}} = \begin{bmatrix} \mathbf{0} \\ -\mathbf{I} \\ \mathbf{I} \\ \mathbf{0} \end{bmatrix}, \quad \mathbf{B}_u = \begin{bmatrix} \mathbf{0} & \mathbf{I} & -\mathbf{I} & \mathbf{0} \end{bmatrix}, \quad \bar{\boldsymbol{\Gamma}} = \begin{bmatrix} \mathbf{0} & -\mathrm{diag}\left(\frac{K}{j\omega} + C\right)^{-1} & \mathbf{0} & \mathbf{0} \end{bmatrix}, \quad \bar{\bar{\boldsymbol{\Omega}}} = \begin{bmatrix} \mathbf{0} & \mathbf{0} & \mathbf{0} & \mathbf{0} \\ \mathbf{0} & \mathbf{0} & \mathbf{0} & \mathbf{0} \\ \mathbf{0} & \mathbf{0} & \mathbf{0} & \mathbf{0} \\ \mathbf{0} & \mathbf{0} & \mathbf{0} & \mathbf{0} \end{bmatrix}. \tag{45}$$

Based on the above, we see that equation 38 reduces to,

$$\mathbf{Y}_C = \mathbf{Y} - \mathbf{Y}\mathbf{B}^{\mathrm{T}} \left[\mathbf{B}\mathbf{Y}\mathbf{B}^{\mathrm{T}} + \mathrm{diag}\left(\frac{K}{j\omega} + C\right)^{-1}\right]^{-1} \mathbf{B}\mathbf{Y} \tag{46}$$

which is the same as the well known result obtained when considering the dual formulation with interface weakening (i.e. a relaxation of compatibility), see for example [21].

4 Numerical example

To verify the hybrid substructuring scheme described through Section 3, and illustrate some of its potential benefits, we present a simple numerical example consisting of end-to-end coupled beams considering translational and rotational DoFs. An illustration of the example is shown in Figure 2. Two free-free beams (A and B) are coupled end-to-end through a junction J. This junction is itself composed two identical beams coupled end-to-end. The individual junction

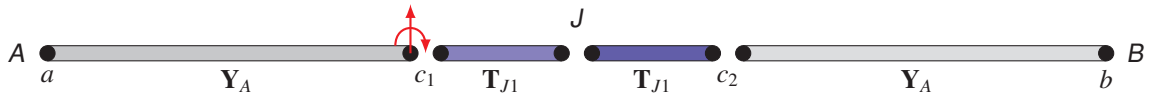

Fig. 2: Illustration of numerical example. Four free-free beams coupled end-to-end (including translational and rotational DoFs at each connection). The central two beams (in blue) represent the AB junction J, and are characterised individually by the transfer matrix $\mathbf{T}_{J1}$.

Table 1: Material properties (Young's modulus E, density ρ and structural damping η) and beam geometries (length L, width W and height H) used for numerical example.

Component	E (Nm^{-2})	ρ (kgm^{-1})	η (-)	$L \times W \times H$ (m)
A	2×10^9	7000	0.05	$0.4 \times 0.03 \times 0.01$
B	2×10^9	7000	0.05	$0.4 \times 0.03 \times 0.01$
J1	2×10^9	7000	0.05	$0.2 \times 0.03 \times 0.01$
J2	2×10^7	1000	0.5	$0.02 \times 0.03 \times 0.001$

beams are described by their transfer matrix $\mathbf{T}_{J1}$, and the entire junction by the coupled transfer matrix $\mathbf{T}_{J11} = \mathbf{T}_{J1}\mathbf{T}_{J1}$. We will also consider a second example, not shown in Figure 2, where a third beam is installed in the junction such that $\mathbf{T}_{J121} = \mathbf{T}_{J1}\mathbf{T}_{J2}\mathbf{T}_{J1}$, where *J2* differs in material properties and geometry to *A, B* and *J1*.

A conventional dual substructuring formulation of this problem would require the admittance matrix of each component to be added to the block diagonal matrix $\mathbf{Y}$, and an appropriate Boolean matrix $\mathbf{B}$ defined that correctly co-locates all coupling DoFs (including c_1 and c_2, but also any internal DoFs within the junction itself). A reconfiguration of the junction, for example adding or remove a component, would thus require we redefining both $\mathbf{Y}$ and $\mathbf{B}$.

For the two and three component junctions (*J11* and *J121*), $\mathbf{Y}$ and $\mathbf{B}$ take the form,

$$\mathbf{Y} = \begin{bmatrix} \mathbf{Y}_A & & & \\ & \mathbf{Y}_{J1} & & \\ & & \mathbf{Y}_{J1} & \\ & & & \mathbf{Y}_B \end{bmatrix} \quad \text{with} \quad \mathbf{B} = \begin{bmatrix} \mathbf{0} & \mathbf{I} & -\mathbf{I} & \mathbf{0} & \mathbf{0} & \mathbf{0} & \mathbf{0} & \mathbf{0} \\ \mathbf{0} & \mathbf{0} & \mathbf{0} & \mathbf{I} & -\mathbf{I} & \mathbf{0} & \mathbf{0} & \mathbf{0} \\ \mathbf{0} & \mathbf{0} & \mathbf{0} & \mathbf{0} & \mathbf{0} & \mathbf{I} & -\mathbf{I} & \mathbf{0} \end{bmatrix} \tag{47}$$

and

$$\mathbf{Y} = \begin{bmatrix} \mathbf{Y}_A & & & & \\ & \mathbf{Y}_{J1} & & & \\ & & \mathbf{Y}_{J2} & & \\ & & & \mathbf{Y}_{J1} & \\ & & & & \mathbf{Y}_B \end{bmatrix} \quad \text{with} \quad \mathbf{B} = \begin{bmatrix} \mathbf{0} & \mathbf{I} & -\mathbf{I} & \mathbf{0} & \mathbf{0} & \mathbf{0} & \mathbf{0} & \mathbf{0} & \mathbf{0} & \mathbf{0} \\ \mathbf{0} & \mathbf{0} & \mathbf{0} & \mathbf{I} & -\mathbf{I} & \mathbf{0} & \mathbf{0} & \mathbf{0} & \mathbf{0} & \mathbf{0} \\ \mathbf{0} & \mathbf{0} & \mathbf{0} & \mathbf{0} & \mathbf{0} & \mathbf{I} & -\mathbf{I} & \mathbf{0} & \mathbf{0} & \mathbf{0} \\ \mathbf{0} & \mathbf{0} & \mathbf{0} & \mathbf{0} & \mathbf{0} & \mathbf{0} & \mathbf{0} & \mathbf{I} & -\mathbf{I} & \mathbf{0} \end{bmatrix}, \tag{48}$$

respectively. With the hybrid admittance-TM coupling, only the end components A and B are included in the block diagonal $\mathbf{Y}$; the junction components are accounted for by the generalized coupling constraints. Thus the inputs to the hybrid substructuring scheme are,

$$\mathbf{Y} = \begin{bmatrix} \mathbf{Y}_A & \\ & \mathbf{Y}_B \end{bmatrix} \quad \text{with} \quad \mathbf{T}_{J11} = \mathbf{T}_{J1}\mathbf{T}_{J1} \quad \text{or} \quad \mathbf{T}_{J121} = \mathbf{T}_{J1}\mathbf{T}_{J2}\mathbf{T}_{J1}. \tag{49}$$

Based on the material properties and beam geometries given in Table 1, Figure 3 shows the individual elements (magnitudes only) of the transfer matrices for: the single junction element *J1* (blue), the two element junction *J11* (orange), and the three element junction *J121*. Shown in Figure 4 are the coupled admittances between the translational DoFs at the ends of components *A* and *B* for the two and three element junctions, computed using standard dual formulation and the hybrid admittance-transfer matrix based approach. As expected, the results are in exact agreement.

The convenience of the hybrid scheme becomes evident when investigating more complex junctions. One can readily compute the transfer matrix of an arbitrarily complex junction $\mathbf{T}_J = \mathbf{T}_{J1}\mathbf{T}_{J2}\cdots\mathbf{T}_{JN}$ with no need to redefine the substructuring equations. This might be useful for problems involving the optimisation of layered structures, such as multi-stage isolation platforms.

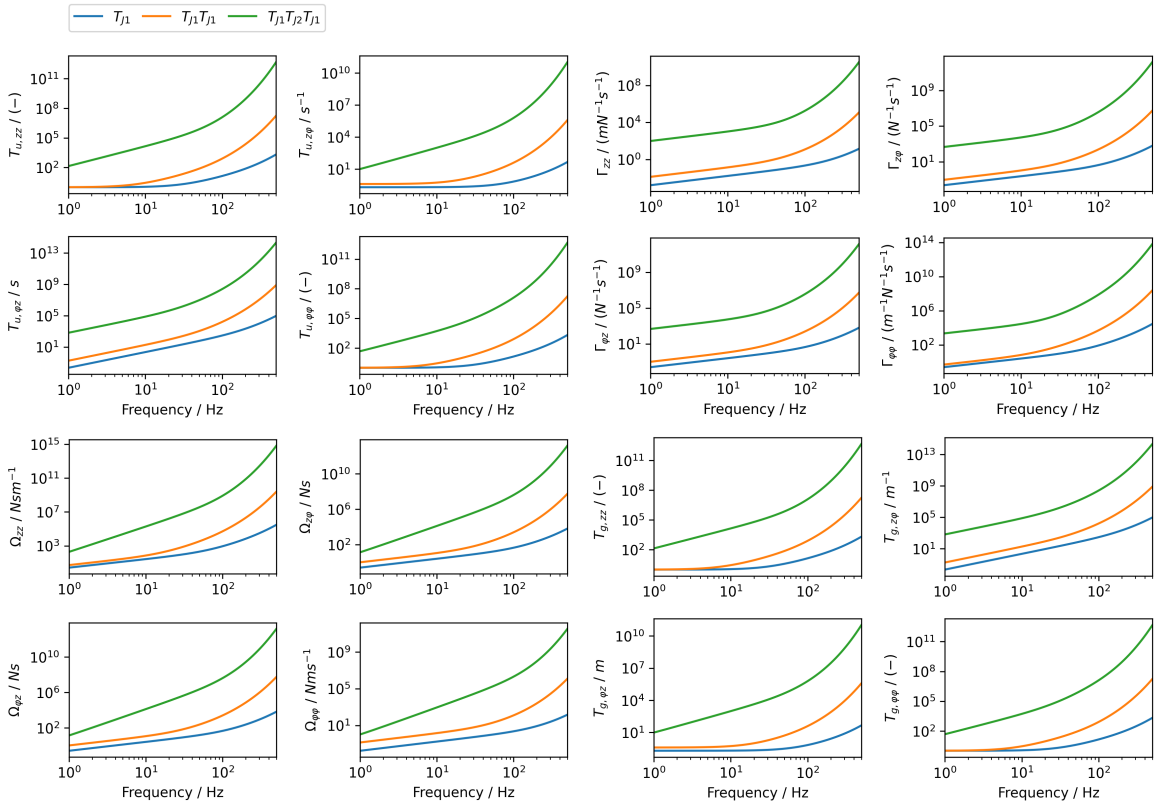

Fig. 3: Transfer matrix for coupled beam junctions: $\mathbf{T}_{J1}$ (blue), $\mathbf{T}_{J11} = \mathbf{T}_{J1}\mathbf{T}_{J1}$ (orange), and $\mathbf{T}_{J121} = \mathbf{T}_{J1}\mathbf{T}_{J2}\mathbf{T}_{J1}$ (green).

4.1 Error analysis

To investigate the sensitivity of the hybrid admittance-transfer matrix coupling scheme to errors in the component characterisation, we perform a simple Monte Carlo (MC) study. In this, we add random Gaussian noise to all component admittance matrices, including those used to compute the joint transfer matrices, according to,

$$\mathbf{Y}_{\square,\text{noisy}} = \mathbf{Y}_{\square} + \mathbf{Y}_{\square}(\mathcal{N}(\mathbf{0}, \epsilon\mathbf{I}) + i\mathcal{N}(\mathbf{0}, \epsilon\mathbf{I})) \tag{50}$$

where the noise variance is set to $\epsilon = 1 \times 10^{-5}$, before being scaled accordingly by the admittance; this ensures the relative variance across the frequency range is constant. The noisy FRFs are then used to compute the coupled admittance via both hybrid and dual substructuring schemes. This process is repeated for 5000 realisations and the standard deviation computed per frequency.

Shown in Figure 5 are the standard deviations of the coupled admittance between the translational DoFs at the ends of components *A* and *B* for the two and three element junctions, computed using the hybrid admittance-transfer matrix and dual methods. If we consider the total standard deviation across all coupled FRFs and all frequencies, for the *A-J1-J1-B* assembly the dual and hybrid methods yield errors or $\sigma_{\text{dual}} = 8.04 \times 10^{-13}$ and $\sigma_{\text{hybrid}} = 7.79 \times 10^{-13}$, respectively. For the *A-J1-J2-J1-B* assembly, we have $\sigma_{\text{dual}} = 3.38 \times 10^{-12}$ and $\sigma_{\text{hybrid}} = 3.53 \times 10^{-12}$. The results indicate that the hybrid scheme is not unduly sensitive to errors in the component characterisations, even when these are compounded through the junction transfer matrix computation. Of course, further studies are required to fully understand the error propagation characteristics of the hybrid scheme.

5 Conclusions

Substructuring is an important step in the analysis of complex built-up structures, with formulations existing in the physical, modal, state, time and frequency domains. In the frequency domain, admittance-based substructuring has become the preferred approach, especially when dealing with components that are characterised experimentally. An alternative approach is the transfer matrix method (TMM). With the TMM, structural components are represented by

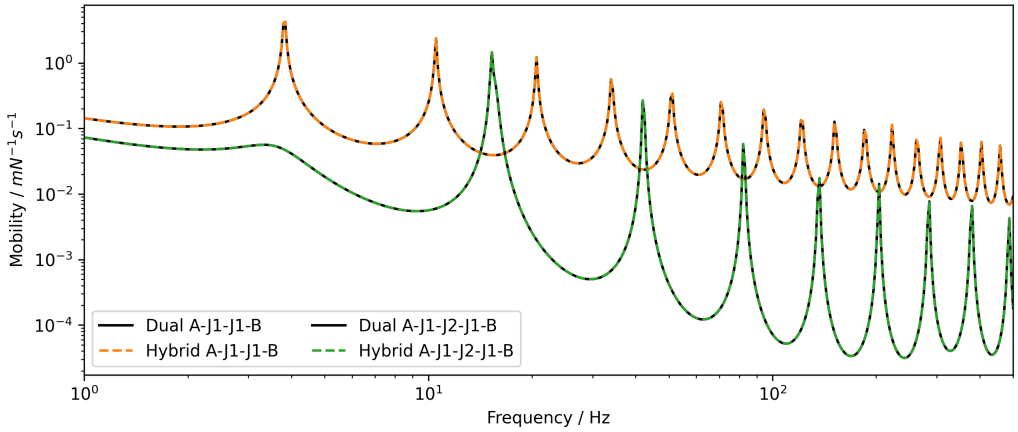

Fig. 4: Coupled mobility of *A-J1-J1-B* (orange) and *A-J1-J2-J1-B* (green) assemblies compared against standard dual formulation.

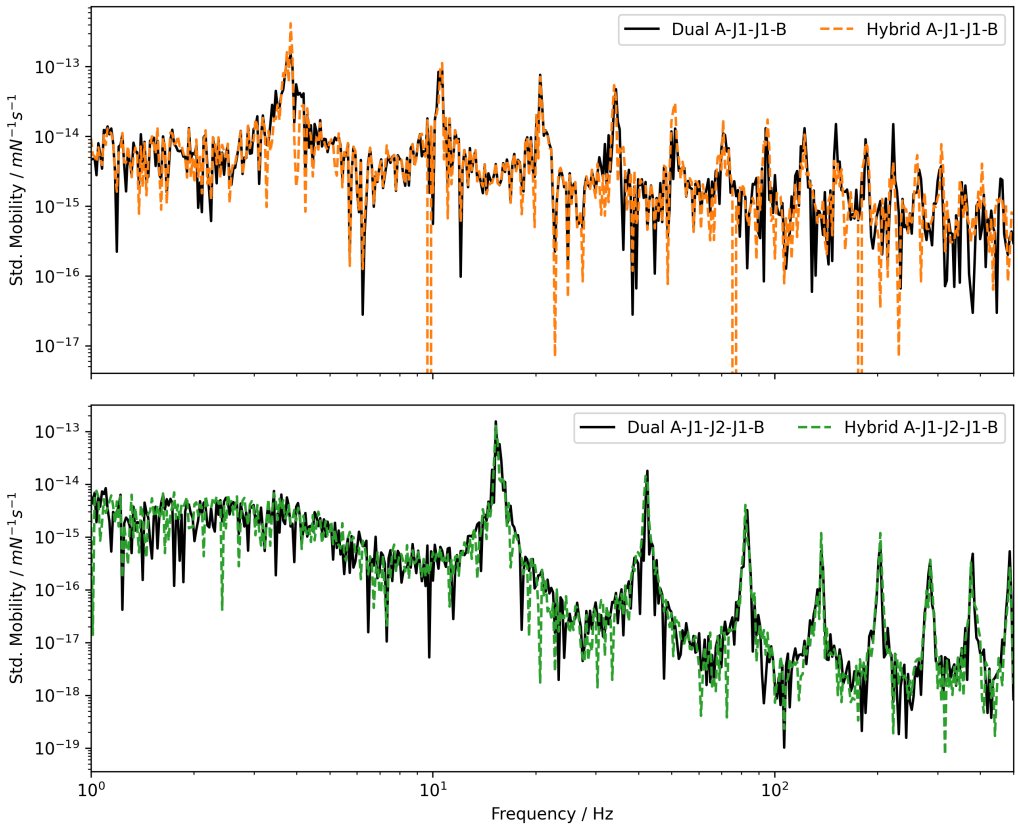

Fig. 5: Standard deviation of the coupled mobility based on Monte-Carlo simulation with random Gaussian noise added to all component admittances (see 50). Top: *A-J1-J1-B* assembly. Bottom: *A-J1-J2-J1-B* assembly.

their *transfer matrices* (TMs) and coupling is achieved simply by multiplying the TMs of the respective components together; there is no need to define any Boolean matrices to co-locate coupling DoFs. This makes the TMM especially convenient when dealing with periodic or complex layered structures, where TMs can be easily combined into arbitrary configurations.

In the present paper we formulate a hybrid substructuring scheme that enables the coupling of admittance-based components by an arbitrarily complex 'junction', whose dynamics are represented by a transfer matrix. This approach allows for the convenient manipulation of the coupling junction (e.g. adding, removing or reordering components) by directly manipulating the product of their transfer matrices. The result is a generalization of the dual substructuring

formulation; the standard Boolean coupling matrices are replaced with force and response transmissibilties and additional force-response coupling terms are introduced.

The method is verified by simple numerical model consisting of end-to-end coupled beams, showing exact agreement with standard dual formulation. Monte-calro simulations are also performed to investigate the sensitivity of the hybrid scheme to errors in the component characterisations, showing comparable performance to standard dual substructuring. Experimental validation and further numerical studies are ongoing, including the investigation of junctions composed of components characterised experimentally.

Appendix

A Transfer matrix representation

The dynamics of a general linear time invariant mechanical system can be described by the following equation of motion,

$$\begin{pmatrix} \mathbf{f}_{c_1} + \mathbf{g}_{c_1} \\ \mathbf{f}_{c_2} + \mathbf{g}_{c_2} \end{pmatrix} = \begin{bmatrix} \mathbf{Z}_{c_1c_1} & \mathbf{Z}_{c_1c_2} \\ \mathbf{Z}_{c_2c_1} & \mathbf{Z}_{c_2c_2} \end{bmatrix} \begin{pmatrix} \mathbf{u}_{c_1} \\ \mathbf{u}_{c_2} \end{pmatrix} \tag{A.1}$$

where $\mathbf{Z}_{\square}$ denotes the mechanical impedance at/between the subscripted DoFs.

We are interested in the transference of force and displacement across a component. Ignoring external force terms, equation A.1 can be rearranged to yield transfer-style matrix as follows. Using the top line of equation A.1 find $\mathbf{u}_b$,

$$\mathbf{g}_{c_1} = \mathbf{Z}_{c_1c_1}\mathbf{u}_{c_1} + \mathbf{Z}_{c_1c_2}\mathbf{u}_{c_2} \rightarrow \mathbf{u}_{c_2} = \mathbf{Z}_{c_1c_2}^{-1}\left(\mathbf{g}_{c_1} - \mathbf{Z}_{c_1c_2}\mathbf{u}_{c_1}\right). \tag{A.2}$$

Substitute $\mathbf{u}_{c_2}$ into $\mathbf{g}_{c_2}$ (second line of equation A.1),

$$\begin{aligned} \mathbf{g}_{c_2} &= \mathbf{Z}_{c_2c_1}\mathbf{u}_{c_1} + \mathbf{Z}_{c_2c_2}\mathbf{u}_{c_2} && \text{(A.3)} \\ &= \mathbf{Z}_{c_2c_1}\mathbf{u}_{c_1} + \mathbf{Z}_{c_2c_2}\left(\mathbf{Z}_{c_1c_2}^{-1}\left(\mathbf{g}_{c_1} - \mathbf{Z}_{c_1c_1}\mathbf{u}_{c_1}\right)\right) && \text{(A.4)} \\ &= \mathbf{Z}_{c_2c_1}\mathbf{u}_{c_1} + \mathbf{Z}_{c_2c_2}\mathbf{Z}_{c_1c_2}^{-1}\mathbf{g}_{c_1} - \mathbf{Z}_{c_2c_2}\mathbf{Z}_{c_1c_2}^{-1}\mathbf{Z}_{c_1c_1}\mathbf{u}_{c_1}. && \text{(A.5)} \end{aligned}$$

After grouping terms we have the following pair of equations,

$$\mathbf{u}_{c_2} = \mathbf{Z}_{c_1c_2}^{-1}\mathbf{g}_{c_1} - \mathbf{Z}_{c_1c_2}^{-1}\mathbf{Z}_{c_1c_1}\mathbf{u}_{c_1} \tag{A.6}$$

$$\mathbf{g}_{c_2} = \left(\mathbf{Z}_{c_2c_1} - \mathbf{Z}_{c_2c_2}\mathbf{Z}_{c_1c_2}^{-1}\mathbf{Z}_{c_1c_1}\right)\mathbf{u}_{c_1} + \mathbf{Z}_{c_2c_2}\mathbf{Z}_{c_1c_2}^{-1}\mathbf{g}_{c_1} \tag{A.7}$$

or in matrix form,

$$\begin{pmatrix} \mathbf{u}_{c_2} \\ \mathbf{g}_{c_2} \end{pmatrix} = \begin{bmatrix} -\mathbf{Z}_{c_1c_2}^{-1}\mathbf{Z}_{c_1c_1} & \mathbf{Z}_{c_1c_2}^{-1} \\ \mathbf{Z}_{c_2c_1} - \mathbf{Z}_{c_2c_2}\mathbf{Z}_{c_1c_2}^{-1}\mathbf{Z}_{c_1c_1} & \mathbf{Z}_{c_2c_2}\mathbf{Z}_{c_1c_2}^{-1} \end{bmatrix} \begin{pmatrix} \mathbf{u}_{c_1} \\ \mathbf{g}_{c_1} \end{pmatrix}. \tag{A.8}$$

Equation A.8 describes the transmission of force and displacement across the component. Its terms can be calculated analytically for simple components (e.g. spring dash-pot joints, beam elements, etc.) or numerically for more complex cases. The transfer matrix is often written in a slightly modified form, with the force $\mathbf{g}_b$ negated,

$$\begin{pmatrix} \mathbf{u}_{c_2} \\ -\mathbf{g}_{c_2} \end{pmatrix} = \begin{bmatrix} -\mathbf{Z}_{c_1c_2}^{-1}\mathbf{Z}_{c_1c_1} & \mathbf{Z}_{c_1c_2}^{-1} \\ -\mathbf{Z}_{c_2c_1} + \mathbf{Z}_{c_2c_2}\mathbf{Z}_{c_1c_2}^{-1}\mathbf{Z}_{c_1c_1} & -\mathbf{Z}_{c_2c_2}\mathbf{Z}_{c_1c_2}^{-1} \end{bmatrix} \begin{pmatrix} \mathbf{u}_{c_1} \\ \mathbf{g}_{c_1} \end{pmatrix} = \begin{bmatrix} \mathbf{T}^u & \mathbf{\Gamma} \\ \mathbf{\Omega} & \mathbf{T}^g \end{bmatrix} \begin{pmatrix} \mathbf{u}_{c_1} \\ \mathbf{g}_{c_1} \end{pmatrix}, \tag{A.9}$$

where we introduce the force and response transmissibilities, respectively, as $\mathbf{T}_u$ and $\mathbf{T}_g$, and the cross-terms as $\mathbf{\Gamma}$ and $\mathbf{\Omega}$. This negation reduces the coupling of components to a simple matrix multiplication.

Direct measurement of the transfer or impedance sub-matrices is generally not possible as both require physically constraining some set of response DoFs [22]. Much like how the impedance matrix can be computed from measured admittance FRFs through inversion, the transfer matrix can similarly be described in-terms of admittance by following a similar procedure as above, though starting from the equation of motion,

$$\begin{pmatrix} \mathbf{u}_{c_1} \\ \mathbf{u}_{c_2} \end{pmatrix} = \begin{bmatrix} \mathbf{Y}_{c_1c_1} & \mathbf{Y}_{c_1c_2} \\ \mathbf{Y}_{c_2c_1} & \mathbf{Y}_{c_2c_2} \end{bmatrix} \begin{pmatrix} \mathbf{f}_{c_1} + \mathbf{g}_{c_1} \\ \mathbf{f}_{c_2} + \mathbf{g}_{c_2} \end{pmatrix}. \tag{A.10}$$

The result is,

$$\begin{pmatrix} \mathbf{u}_{c_2} \\ -\mathbf{g}_{c_2} \end{pmatrix} = \begin{bmatrix} \mathbf{T}^u & \mathbf{\Gamma} \\ \mathbf{\Omega} & \mathbf{T}^g \end{bmatrix} \begin{pmatrix} \mathbf{u}_{c_1} \\ \mathbf{g}_{c_1} \end{pmatrix} = \begin{bmatrix} \mathbf{Y}_{c_2c_2}\mathbf{Y}_{c_1c_2}^{-1} & \mathbf{Y}_{c_2c_1} - \mathbf{Y}_{c_2c_2}\mathbf{Y}_{c_1c_2}^{-1}\mathbf{Y}_{c_1c_1} \\ -\mathbf{Y}_{c_1c_2}^{-1} & \mathbf{Y}_{c_1c_2}^{-1}\mathbf{Y}_{c_1c_1} \end{bmatrix} \begin{pmatrix} \mathbf{u}_{c_1} \\ \mathbf{g}_{c_1} \end{pmatrix}. \tag{A.11}$$

The advantage of this admittance-based transfer matrix representation is that all terms can be obtained from experimental measurements without the need to first compute the impedance matrix.

References

[1] J. Meggitt and A. Moorhouse. *Experimental Vibro-acoustics: In situ and blocked force methods for component-based simulation and virtual prototyping*. CRC Press, 2025.

[2] D. De Klerk, D. J. Rixen, and S. N. Voormeeren. General framework for dynamic substructuring: history, review and classification of techniques. *AIAA journal*, 46(5):1169–1181, 2008.

[3] W. D'Ambrogio and A. Fregolent. Inverse dynamic substructuring using the direct hybrid assembly in the frequency domain. *Mechanical Systems and Signal Processing*, 45(2):360–377, 2014.

[4] S. Rubin. Mechanical immittance-and transmission-matrix concepts. *The Journal of the Acoustical Society of America*, 41(5): 1171–1179, 1967.

[5] V. Yildirim, E. Sancaktar, and E. Kiral. Free vibration analysis of symmetric cross-ply laminated composite beams with the help of the transfer matrix approach. *Communications in Numerical Methods in Engineering*, 15(9):651–660, 1999.

[6] Y. Song, J. Wen, D. Yu, Y. Liu, and X. Wen. Reduction of vibration and noise radiation of an underwater vehicle due to propeller forces using periodically layered isolators. *Journal of Sound and vibration*, 333(14):3031–3043, 2014.

[7] W. Lauriks, P. Mees, and J. F. Allard. The acoustic transmission through layered systems. *Journal of sound and vibration*, 155 (1):125–132, 1992.

[8] B. Brouard, D. Lafarge, and J.-F. Allard. A general method of modelling sound propagation in layered media. *Journal of Sound and Vibration*, 183(1):129–142, 1995.

[9] J. Massaglia. *Modelling the sound insulation of corrugated roof structures: an extended transfer matrix approach*. University of Salford (United Kingdom), 2017.

[10] M. Boiangiu, V. Ceausu, and C. D. Untaroiu. A transfer matrix method for free vibration analysis of euler-bernoulli beams with variable cross section. *Journal of Vibration and Control*, 22(11):2591–2602, 2016.

[11] J. W. Lee and J. Y. Lee. Free vibration analysis using the transfer-matrix method on a tapered beam. *Computers & Structures*, 164:75–82, 2016.

[12] D. Pearson. The transfer matrix method for the vibration of compressed helical springs. *Journal of Mechanical Engineering Science*, 24(4):163–171, 1982.

[13] S.-C. Hsieh, J.-H. Chen, and A.-C. Lee. A modified transfer matrix method for the coupling lateral and torsional vibrations of symmetric rotor-bearing systems. *Journal of Sound and Vibration*, 289(1-2):294–333, 2006.

[14] C.-Y. Tsai and S.-C. Huang. Transfer matrix method to vibration analysis of rotors with coupler offsets. *Shock and vibration*, 20(1):97–108, 2013.

[15] L. Sun, A. Leung, Y. Lee, and K. Song. Vibrational power-flow analysis of a mimo system using the transmission matrix approach. *Mechanical systems and signal processing*, 21(1):365–388, 2007.

[16] M. Dokainish. A new approach for plate vibrations: combination of transfer matrix and finite-element technique. *Journal of Engineering for Industry*, 94(2):526–530, 1972.

[17] C. Decraene, A. Dijckmans, and E. P. Reynders. Fast mean and variance computation of the diffuse sound transmission through finite-sized thick and layered wall and floor systems. *Journal of Sound and Vibration*, 422:131–145, 2018.

[18] F. Chevillotte and R. Panneton. Coupling transfer matrix method to finite element method for analyzing the acoustics of complex hollow body networks. *Applied Acoustics*, 72(12):962–968, 2011.

[19] D. Duhamel, B. R. Mace, and M. J. Brennan. Finite element analysis of the vibrations of waveguides and periodic structures. *Journal of sound and vibration*, 294(1-2):205–220, 2006.

[20] N. Maia, A. Urgueira, and R. Almeida. Whys and wherefores of transmissibility. *Vibration Analysis and Control: New Trends and Developments*, page 197, 2011.

[21] A. E. Mahmoudi, D. J. Rixen, and C. H. Meyer. Comparison of different approaches to include connection elements into frequency-based substructuring. *Experimental Techniques*, 44(4):425–433, 2020.

[22] J.-Y. Ha and K.-J. Kim. Analysis of mimo mechanical systems using the vectorial four pole parameter method. *Journal of Sound and Vibration*, 180(2):333–350, 1995.